

## Targeted trace ingredients coupled with chemometric analysis for consistency evaluation of *Panax notoginseng* saponins injectable formulations

Jingxian ZHANG, Zijia ZHANG, Zhaojun WANG, Tengqian ZHANG, Yang ZHOU, Ming CHEN, Zhanwen HUANG, Qingqing HE, Huali LONG, Jinjun HOU, Wanying WU, Dean GUO

**Citation:** Jingxian ZHANG, Zijia ZHANG, Zhaojun WANG, Tengqian ZHANG, Yang ZHOU, Ming CHEN, Zhanwen HUANG, Qingqing HE, Huali LONG, Jinjun HOU, Wanying WU, Dean GUO, Targeted trace ingredients coupled with chemometric analysis for consistency evaluation of *Panax notoginseng* saponins injectable formulations, *Chinese Journal of Natural Medicines*, 2023, 21(8), 631–640. doi: [10.1016/S1875-5364\(23\)60396-6](https://doi.org/10.1016/S1875-5364(23)60396-6).

View online: [https://doi.org/10.1016/S1875-5364\(23\)60396-6](https://doi.org/10.1016/S1875-5364(23)60396-6)

## Related articles that may interest you

*Panax notoginseng* saponins prevent colitis-associated colorectal cancer development: the role of gut microbiota

Chinese Journal of Natural Medicines. 2020, 18(7), 500–507 [https://doi.org/10.1016/S1875-5364\(20\)30060-1](https://doi.org/10.1016/S1875-5364(20)30060-1)

*Panax notoginseng* saponins prevent colitis-associated colorectal cancer via inhibition IDO1 mediated immune regulation

Chinese Journal of Natural Medicines. 2022, 20(4), 258–269 [https://doi.org/10.1016/S1875-5364\(22\)60179-1](https://doi.org/10.1016/S1875-5364(22)60179-1)

Metabolomics analysis reveals the renal protective effect of *Panax ginseng* C. A. Mey in type 1 diabetic rats

Chinese Journal of Natural Medicines. 2022, 20(5), 378–386 [https://doi.org/10.1016/S1875-5364\(22\)60175-4](https://doi.org/10.1016/S1875-5364(22)60175-4)

Integrative SMRT sequencing and ginsenoside profiling analysis provide insights into the biosynthesis of ginsenoside in *Panax quinquefolium*

Chinese Journal of Natural Medicines. 2022, 20(8), 614–626 [https://doi.org/10.1016/S1875-5364\(22\)60198-5](https://doi.org/10.1016/S1875-5364(22)60198-5)

Five new spirosterol saponins from *Allii Macrostemonis Bulbus*

Chinese Journal of Natural Medicines. 2023, 21(3), 226–232 [https://doi.org/10.1016/S1875-5364\(23\)60423-6](https://doi.org/10.1016/S1875-5364(23)60423-6)

Advances on hormone-like activity of *Panax ginseng* and ginsenosides

Chinese Journal of Natural Medicines. 2020, 18(7), 526–535 [https://doi.org/10.1016/S1875-5364\(20\)30063-7](https://doi.org/10.1016/S1875-5364(20)30063-7)



Wechat

•Original article•

## Targeted trace ingredients coupled with chemometric analysis for consistency evaluation of *Panax notoginseng* saponins injectable formulations

ZHANG Jingxian<sup>2Δ</sup>, ZHANG Zijia<sup>1,4Δ</sup>, WANG Zhaojun<sup>1,4</sup>, ZHANG Tengqian<sup>1,4</sup>, ZHOU Yang<sup>1,4</sup>,  
CHEN Ming<sup>3</sup>, HUANG Zhanwen<sup>3</sup>, HE Qingqing<sup>1,4</sup>, LONG Huali<sup>1,4</sup>, HOU Jinjun<sup>1,4\*</sup>,  
WU Wanying<sup>1,4\*</sup>, GUO Dean<sup>1,4\*</sup>

<sup>1</sup> National Engineering Research Center of TCM Standardization Technology, Shanghai Institute of Materia Medica, Chinese Academy of Sciences, Shanghai 201203, China;

<sup>2</sup> NMPA Key Laboratory for Quality Control of Traditional Chinese Medicine, Shanghai Institute for Food and Drug Control, Shanghai 201203, China;

<sup>3</sup> Guangxi Key Laboratory of Comprehensive Utilization Technology of Pseudo-Ginseng, Guangxi Zhongheng Innovative Pharmaceutical Research Co., Ltd., Guangxi 530032, China;

<sup>4</sup> School of Pharmacy, University of Chinese Academy of Sciences, Beijing 100049, China

Available online 20 Aug., 2023

**[ABSTRACT]** Evaluating the consistency of herb injectable formulations could improve their product quality and clinical safety, particularly concerning the composition and content levels of trace ingredients. *Panax notoginseng* Saponins Injection (PNSI), widely used in China for treating acute cardiovascular diseases, contains low-abundance (10%–25%) and trace saponins in addition to its five main constituents (notoginsenoside R<sub>1</sub>, ginsenoside Rg<sub>1</sub>, ginsenoside Re, ginsenoside Rb<sub>1</sub>, and ginsenoside Rd). This study aimed to establish a robust analytical method and assess the variability in trace saponin levels within PNSI from different vendors and formulation types. To achieve this, a liquid chromatography-triple quadrupole mass spectrometry (LC-MS/MS) method employing multiple ions monitoring (MIM) was developed. A “post-column valve switching” strategy was implemented to eliminate highly abundant peaks (NR<sub>1</sub>, Rg<sub>1</sub>, and Re) at 26 min. A total of 51 saponins in PNSI were quantified or relatively quantified using 18 saponin standards, with digoxin as the internal standard. This study evaluated 119 batches of PNSI from seven vendors, revealing significant variability in trace saponin levels among different vendors and formulation types. These findings highlight the importance of consistent content in low-abundance and trace saponins to ensure product control and clinical safety. Standardization of these ingredients is crucial for maintaining the quality and effectiveness of PNSI in treating acute cardiovascular diseases.

**[KEY WORDS]** Consistency evaluation; *Panax notoginseng* saponins; PCA analysis; Xueshuantong; Xuesaitong

**[CLC Number]** R917    **[Document code]** A    **[Article ID]** 2095-6975(2023)08-0631-10

**[Received on]** 29-Mar.-2023

**[Research funding]** This work was supported by the Science and Technology Service Network Initiative of the Chinese Academy of Sciences (STS, No. KFJ-STS-QYZD-2021-03-003), the Construction Projects of the Research Center for Notoginseng Health Products by the Department of Science and Technology of Guangxi Province (No. AD20297068), and the Sanming Project of Medicine in Shenzhen (No. SZZYSM202106004).

**[\*Corresponding author]** E-mails: jinjun\_hou@sim.ac.cn (HOU Jinjun); wanyingwu@sim.ac.cn (WU Wanying); daguo@sim.ac.cn (GUO Dean)

<sup>Δ</sup>These authors contributed equally to this work.

These authors have no conflict of interest to declare.

### Introduction

Product consistency of parenteral products, especially injectable herbal drugs, is one of the most intractable challenges faced by the pharmaceutical industry [1]. While these drugs are predominantly manufactured and distributed in China, the demand for evaluating product consistency has driven the development of novel analytical techniques to enhance quality control and ensure clinical safety. For example, the fingerprint chromatogram technique has been employed to monitor the chromatographic profile consistency of comprehensive chemical ingredients [2–4], and the quantitative analysis of multi-components by single marker (QAMS) technique was developed for primary chemical ingredients in injectable

tions [5, 6]. Furthermore, the liquid chromatography-triple quadrupole mass spectrometry (LC-MS/MS) technique has been applied for the quantitative analysis of various chemical ingredients [7, 8].

*Panax notoginseng* Saponins Injection (PNSI) is mainly comprised of *Panax notoginseng* saponins, which are extracted and purified from the rhizome or taproot of *Panax notoginseng* (Burk.) F.H. Chen (Araliaceae) [9]. It is widely used in China for improving blood circulation in cardiovascular diseases, such as atherosclerotic thrombotic cerebral infarction, cerebral embolism, central retinal vein occlusion, and diabetic kidney disease [1, 10-15]. Based on the formulation type and different root parts of *Panax notoginseng* as the raw materials, the PNSI could be divided into Xueshuantong lyophilized powder for injection (PNSI-1), Xueshuantong injection solution (PNSI-2), Xuesaitong lyophilized powder for injection (PNSI-3), and Xuesaitong injection solution (PNSI-4). PNSI-1 and PNSI-2 were prepared with the taproot of *Panax notoginseng*, while PNSI-3 and PNSI-4 were prepared with the rhizome part of *Panax notoginseng* [16]. With at least seven vendors involved in the production and distribution of PNSI products, it is imperative to conduct a thorough investigation to assess and establish product consistency across different PNSI formulations.

The PNSI formulation primarily comprises five key dammarane-type triterpenoid saponins: notoginsenoside R<sub>1</sub>, ginsenoside Rg<sub>1</sub>, ginsenoside Re, ginsenoside Rb<sub>1</sub>, and ginsenoside Rd [17]. These saponins collectively contribute to approximately 75% to 90% of the total saponin content (unpublished data from our laboratory). Interestingly, the total content levels of these five saponins were found to be lower in Xuesaitong than that in Xueshuantong. Our previous study developed an ultra-high performance liquid chromatography (UHPLC) with quadrupole time-of-flight MS-based metabolomics approach to probe the saponin discrimination between Xueshuantong and Xuesaitong products [18]. Our analysis detected a total of 148 distinct triterpenoid saponins in PNSI, with varying contributions from the five main saponins to the observed variations among the PNSI samples. However, a comprehensive method for evaluating the consistency of trace saponins in PNSI is currently lacking.

LC-MS/MS technique has been the “gold standard” for quantifying the trace chemical ingredients in samples [19]. However, the high-abundance ingredients usually bring peak contamination when detecting trace ingredients [20]. Thus, to quantify the trace saponins in PNSI, a post-column valve switching strategy combined with high sample concentrate was adopted to remove the high-abundance saponins and increase the response of trace saponins. Together with previous studies, 51 trace saponins were quantified or relatively quantified with 18 saponins standards. To perform the consistency evaluation of the PNSI, a total of 119 batches of PNSI from seven different vendors were analyzed with PCA analysis.

## Materials and Methods

### Materials

A total of 23 saponin standards were employed in this study, including notoginsenoside-R<sub>3</sub> (1), -R<sub>1</sub>, 20S-R<sub>2</sub> (31), -K (44), ginsenoside-Rg<sub>1</sub>, -Re, -Rb<sub>1</sub>, -Rd, 20-gluco-Rf (4), -Rf (26), -Rg<sub>2</sub> (35), 20S-Rh<sub>1</sub> (36), -Rc (37), 20R-Rh<sub>1</sub> (38), -Rb<sub>2</sub> (39), F<sub>2</sub> (45), 20S-Rg<sub>3</sub> (49), -Rh<sub>4</sub> (47), 5,6-didehydroginsenoside Rb<sub>1</sub> (30), 20S-sanchirrhinoside A<sub>3</sub> (16) were purchased from Shanghai Standards Biotech Co., Ltd. (Shanghai, China). Ginsenoside F<sub>1</sub> (42) was obtained from National Institutes for Food and Drug Control (Beijing, China). Ginsenoside Rb<sub>3</sub> (40) was provided by the Kunming Institute of Botany, Chinese Academy of Sciences. Ginsenoside Rk<sub>1</sub> (50) was purchased from Shanghai Pureone Biotechnology Co., Ltd. (Shanghai, China). The 18 saponin standards used for quantitation were carefully selected, and their structural and purity information is provided in Table S1 and Fig. S1. The analysis is involved the use of 9 PPT-type saponins, 7 PPD-type saponins, and 2 C17-side chains varied type saponins. Additionally, digoxin (purity > 98.0%) from J&K Scientific (Beijing, China) was employed as the internal standard (IS).

A total of 119 batches of PNSI were prepared by seven different vendors and were categorized into five groups (Table S2). PNSI-1 (60 batches, vendor 1, Lyophilized powder for injection), PNSI-2 (22 batches, vendor 1, Injection solvent), and PNSI-5 (14 batches, vendor 5/6/7, Injection solvent) were made of *Panax notoginseng* saponins from the root (taproot) of *Panax notoginseng*. PNSI-3 (10 batches, vendor 2/3, Lyophilized powder for injection) and PNSI-4 (14 batches, vendor 2/3/4, Injection solvent) were made of *Panax notoginseng* saponins from the rhizome of *Panax notoginseng* (the rhizome and taproot of *P. notoginseng* are shown in Fig. S2). The specifics of those injections were shown in Supporting Information Table S2.

For the chromatographic separation, high-quality LC-MS grade acetonitrile, methanol (Merck, Darmstadt, Germany), and formic acid (Sigma-Aldrich, St Louis, MO, USA) were utilized. Ultrapure water (18.2 MΩ·cm at 25 °C), prepared by a Milli-Q purification system (Millipore, Bedford, USA), served as the mobile phase.

### Sample solution preparation

The PNSI was first prepared as a 1.0 mg·mL<sup>-1</sup> sample stock solution with 50% methanol–water solvent. Precisely, 10 μL of the sample stock solution was transferred into a 1.5 mL centrifuge tube (Eppendorf), followed by the accurate addition of 10 μL of an IS solution (1 mg·mL<sup>-1</sup>). To achieve a final volume, we added 980 μL of 50% methanol–water solvent. The resulting solution was thoroughly mixed using vortexing and then centrifuged at 14 000 r·min<sup>-1</sup> (10 μg·mL<sup>-1</sup>, 10 min, 4 °C).

### Instruments and analytical conditions

The analysis was conducted using an HPLC system (Model 1290, Agilent Technologies, Germany) comprising a binary pump, online degasser, autosampler, column compartment, and diode array detector. The optimal column selected

for the study was the Waters ACQUITY UPLC HSS C<sub>18</sub> column (2.1 mm × 100 mm, 1.8 μm). The mobile phase was composed of waters (A) and acetonitrile (B), and both contained 0.1 mmol·L<sup>-1</sup> ammonium chloride. A gradient elution program was employed with the following profile: 0/8/13/25 min, 20%/21%/27%/53%/90% (B%). The post-column valve was switched to waste at 6.8–7.3 min (to remove NR<sub>1</sub>) and at 9.1–9.8 min (to remove Rg<sub>1</sub> and Re) (Fig. 1) to eliminate interference from specific peaks. The flow rate was set at 0.3 mL·min<sup>-1</sup>, the column temperature was maintained at 25 °C, and the injection volume was 2 μL.

API 4000 triple quadrupole mass spectrometer (Applied Biosystems, Foster City, CA, USA), equipped with a turbo ion spray interface operated in negative ion mode at -4500 V and 550 °C. Gas flow rates for gases 1 (GS1) and 2 (GS2) were set at 50 and 60 L·min<sup>-1</sup>, respectively. The curtain gas (CUR) flow rate was maintained at 20 L·min<sup>-1</sup>, and the collision gas (CAD) flow rate at 4.0 L·min<sup>-1</sup>. Declustering potential (DP) and collision cell exit potential (CXP) are shown in Table 1. The entrance potential (EP) was set to -10 V, collision energy (CE) was set to -5 V, and dwell time was set to 40 ms for all the ions. MIM was used for quantifying the protonated precursor molecular ions [M + Cl]<sup>-</sup>, with both quadrupoles Q1 and Q3 set at unit resolution.

#### Method validation

The method validation procedure included an investigation of intra- and inter-day repeatability, determination of the linear range, assessment of the limit of detection (LOD) and limit of quantitation (LOQ), by performing recovery experiments, wherein standards were added to the samples at levels of 50%, 100%, and 150%. Furthermore, the stability of the sample solutions was assessed over a period of 24 h.

#### Data processing and chemometric analysis

The LC-MS/MS quantitation data were processed by

Analyst Software 1.6.3 (Applied Biosystems, Foster City, CA, USA). The results obtained from the analysis of the 119 batches were processed by Microsoft Office Excel. Principle component analysis (PCA) was performed using SIMCA-P 14.1 (Umetrics, Umea, Sweden), which involved the generation of score plots, biplots, and loading plots. Prior to analysis, all data were scaled using the par method.

## Results and Discussion

### Comprehensive selection of minor panax notoginsenosides in PNSI

There are five main active constituents in PNSI, including notoginsenoside R<sub>1</sub>, ginsenoside Rg<sub>1</sub>, ginsenoside Re, ginsenoside Rb<sub>1</sub>, and ginsenoside Rd, which collectively contribute to 75%–90% of the total composition. The low-abundance and trace saponins take up approximately 10%–25% of the content in PNSI. To ensure accurate quantification of these trace saponins in PNSIs, we performed a comprehensive selection of 51 trace saponins based on their response and significance, as reported in previous literature (Table 1)<sup>[10]</sup>. This selection encompasses 14 classes of [M + Cl]<sup>-</sup> ions and covers all the major trace components in the injection. Among the 51 trace saponins identified, 18 were obtained as reference standards for quantitative and relative quantitation studies (Table S1). Additionally, leveraging high-resolution LC-MS studies and previous research<sup>[18]</sup>, we inferred the structures of 12 additional trace saponins while investigating the saponin types and glycosyl compositions of the remaining 21 trace saponins (Table 1).

### Post-column valve switching technique for developing quantitative methods

The determination of trace saponins in PNSI was performed in the negative ion mode, and 0.1 mmol·L<sup>-1</sup> ammonium chloride was added to the mobile phase to improve the

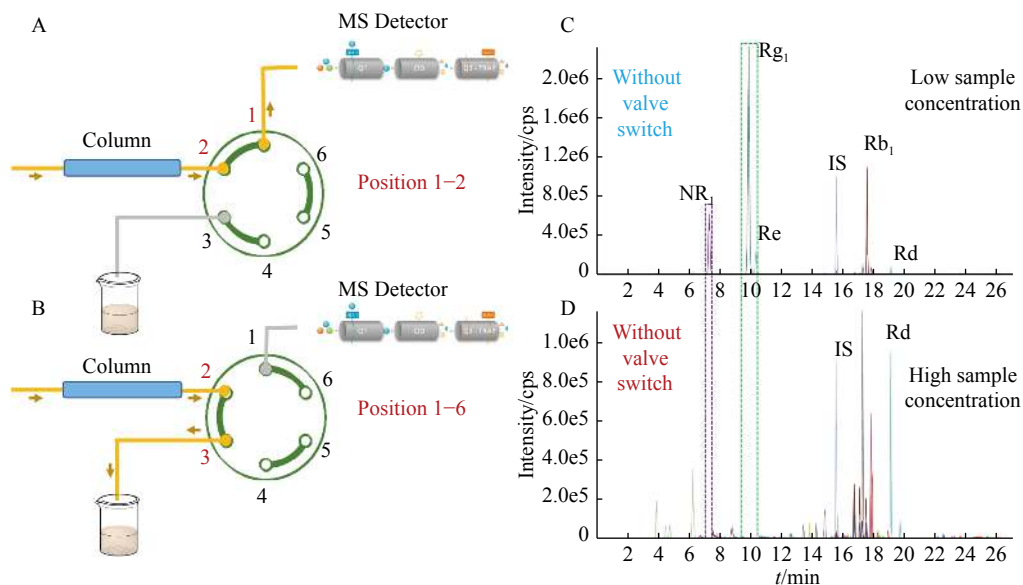


**Fig. 1** Post-column valve switching to remove NR<sub>1</sub>, Rg<sub>1</sub>, and Re in PNSI chromatogram. (A) The six-way valve position 1–2; (B) The six-way valve position 1–6; (C) Multiple ions monitoring (MIM) chromatogram without valve switching (50 μg·mL<sup>-1</sup>); (D) MIM chromatogram with valve switching (0.5 mg·mL<sup>-1</sup>)

**Table 1** The MS parameters of 14 ions used for monitor 51 saponins and the identification of the 51 saponins

No.	$m/z$ [M + Cl] <sup>-</sup>	DP (Volts)	CXP (Volts)	Molecular formula	Standards*	Number of detected ions	$t_R$ /min (compound No.)
1	655.4	-130	-4	C <sub>36</sub> H <sub>60</sub> O <sub>8</sub>	<b>Rh<sub>4</sub></b>	2	22.08 (Rk <sub>3</sub> , <b>46</b> ); 22.48 (Rh <sub>4</sub> , <b>47</b> )
2	673.4	-126	-9	C <sub>36</sub> H <sub>62</sub> O <sub>9</sub>	20(S/R)-Rh <sub>1</sub> /F <sub>1</sub>	3	17.82 (20S-Rh <sub>1</sub> , <b>36</b> ); 18.17 (20R-Rh <sub>1</sub> , <b>38</b> ); 18.87 (F <sub>1</sub> , <b>42</b> )
3	801.5	-157	-10	C <sub>42</sub> H <sub>70</sub> O <sub>12</sub>	<b>Rk<sub>1</sub></b>	2	25.28 (Rk <sub>1</sub> , <b>50</b> ); 25.40 (Rg <sub>5</sub> , <b>51</b> )
4	805.5	-136	-6	C <sub>41</sub> H <sub>70</sub> O <sub>13</sub>	<b>NR<sub>2</sub>/A<sub>3</sub></b>	4	13.36 (A <sub>4</sub> , <b>10</b> ); 14.21 (805-1, <b>14</b> ); 14.76 (A <sub>3</sub> , <b>16</b> ); 17.20 (NR <sub>2</sub> , <b>31</b> ) [805: PPT-Xyl-Glc]
IS	815.5	-140	-10	C <sub>41</sub> H <sub>64</sub> O <sub>14</sub>	Digoxin (IS)	—	15.57
5	819.5	-143	-7	C <sub>42</sub> H <sub>72</sub> O <sub>13</sub>	<b>Rg<sub>2</sub>/20(S)-Rg<sub>3</sub>/F<sub>2</sub></b>	5	15.49 (819-1, <b>20</b> ); 17.76 (Rg <sub>2</sub> , <b>35</b> ); 21.77 (F <sub>2</sub> , <b>45</b> ); 23.04 (20S-Rg <sub>3</sub> , <b>48</b> ); 23.20 (20S-Rg <sub>3</sub> , <b>49</b> ) [819: PPD-Glc-Glc]
6	835.5	-150	-10	C <sub>42</sub> H <sub>72</sub> O <sub>14</sub>	Rf	1	16.70 (Rf, <b>26</b> )
7	967.5	-140	-10	C <sub>47</sub> H <sub>80</sub> O <sub>18</sub>	—	6	8.72 (A <sub>5</sub> , <b>7</b> ); 11.49 (967-1, <b>9</b> ); 15.22 (967-2, <b>18</b> ); 15.55 (967-3, <b>21</b> ); 16.62 (967-4, <b>24</b> ); 17.29 (967-5, <b>32</b> ) [967: PPT-Glc-Glc-Xyl]
8	981.5	-180	-8	C <sub>48</sub> H <sub>82</sub> O <sub>18</sub>	<b>Noto-K</b>	1	19.65 (Noto-K, <b>44</b> )
9	995.5	-151	-6	C <sub>48</sub> H <sub>80</sub> O <sub>19</sub>	—	3	13.40 (995-1 <b>11</b> ); 13.76 (Noto-G, <b>12</b> ); 16.75 (995-2, <b>27</b> ) [995: (7-OH-5-ene-PPD)-Glc-Glc-Glc]
10	997.5	-140	-7	C <sub>48</sub> H <sub>82</sub> O <sub>19</sub>	<b>NR<sub>3</sub>/20-O-glu-Rf</b>	11	3.79 (NR <sub>3</sub> , <b>1</b> ); 4.37 (Re <sub>3</sub> , <b>2</b> ); 4.64 (Noto-M, <b>3</b> ); 6.16 (20-O-glu-Rf, <b>4</b> ); 6.81 (997-1, <b>5</b> ); 7.72 (997-2, <b>6</b> ); 8.83 (997-3, <b>8</b> ); 13.76 (997-4, <b>13</b> ); 14.21 (Vina R <sub>4</sub> , <b>15</b> ); 15.21 (997-5, <b>17</b> ); 15.63 (997-6, <b>22</b> ) [997: PPT-Glc-Glc-Glc]
11	1113.6	-218	-8	C <sub>53</sub> H <sub>90</sub> O <sub>22</sub>	<b>Rb<sub>2</sub>/Rb<sub>3</sub>/Rc</b>	5	17.84 (Rc, <b>37</b> ); 18.24 (Rb <sub>2</sub> , <b>39</b> ); 18.35 (Rb <sub>3</sub> , <b>40</b> ); 18.56 (1113-1, <b>41</b> ); 19.56 (1113-2, <b>43</b> ) [1113: PPD-Glc-Glc-Glc-Xyl]
12	1141.6	-135	-5	C <sub>54</sub> H <sub>90</sub> O <sub>23</sub>	<b>5,6-Didehydro-Rb<sub>1</sub></b>	3	15.31 (isomer of 5,6-didehydro-Rb <sub>1</sub> , <b>19</b> ); 17.20 (5,6-didehydro-Rb <sub>1</sub> , <b>30</b> ); 17.45 (isomer of 5,6-didehydro-Rb <sub>1</sub> , <b>33</b> )
13	1275.6	-173	-8	C <sub>59</sub> H <sub>100</sub> O <sub>27</sub>	—	3	16.67 (1275-1, <b>25</b> ); 17.02 (Ra <sub>3</sub> , <b>28</b> ); 17.45 (isomer of Ra <sub>3</sub> , <b>34</b> ) [1275: PPD-Glc-Glc-Glc-Xyl]
14	1407.6	-140	-15	C <sub>64</sub> H <sub>108</sub> O <sub>31</sub>	—	2	16.24 (Noto-T <b>23</b> ); 17.02 (1407-1, <b>29</b> ) [1407: PPD-Glc-Glc-Xyl-Xyl-(Glc-Xyl)]
Sum					18	51	

\*The bolded saponins were used to determine.

MS response [21]. The molecular ion peaks of the saponins were mainly [M + Cl]<sup>-</sup> in the negative ion mode. The signals of trace components were severely masked by the four high-abundance saponins and were difficult to detect using standard MS technique, since PNS contains a large amount of notoginsenoside R<sub>1</sub> (C<sub>47</sub>H<sub>80</sub>O<sub>18</sub>, [M + Cl]<sup>-</sup>,  $m/z$  967.5, NR<sub>1</sub>), ginsenoside Rg<sub>1</sub> (C<sub>42</sub>H<sub>72</sub>O<sub>14</sub>, [M + Cl]<sup>-</sup>,  $m/z$  835.5, Rg<sub>1</sub>), ginsenoside Re (C<sub>48</sub>H<sub>82</sub>O<sub>18</sub>, [M + Cl]<sup>-</sup>,  $m/z$  981.5, Re), and ginsenoside Rb<sub>1</sub> (C<sub>54</sub>H<sub>92</sub>O<sub>23</sub>, [M + Cl]<sup>-</sup>,  $m/z$  1143.5, Rb<sub>1</sub>) (Fig. 1C). If the injection volume increased, the above four components would exceed their linear detection range. Thus, the four components were not investigated in this study. However, the [M + Cl]<sup>-</sup> ion peaks of NR<sub>1</sub>, Rg<sub>1</sub>, and Re severely overlapped with the trace saponins in PNSIs and could not be eliminated by ion selection. Even with the scheduled MRM approach, a large ion overload still existed on the MS spectra due to the high concentrations of these components. To address this issue, we employed a post-column valve-switching approach to eliminate the inference of NR<sub>1</sub>, Rg<sub>1</sub>, and Re saponins (Figs. 1A, 1B). Briefly,

through the six-way valve after the chromatography column, the peaks of the trace components would enter the MS unit with the mobile phase through the 1–2 position of the six-way valve for detection (Fig. 1A). When NR<sub>1</sub> (6.8–7.3 min), Rg<sub>1</sub> and Re (9.1–9.8 min) peaks arrived, the six-way valve was switched to the 1–6 position (Fig. 1B), and the three components were discharged into the waste collector. The valve was switched back to the 1–2 position after NR<sub>1</sub>, Re, and Rg<sub>1</sub> peaks were over, and the remaining components could enter the MS unit as usual. Little overlap was found between the [M + Cl]<sup>-</sup> ion peak of Rb<sub>1</sub> and the 14 trace saponins listed in Table 1. Besides, a few trace saponin peaks were found near the Rb<sub>1</sub> ion peak on the MS spectra, which limited the application of the valve-switching strategy on Rb<sub>1</sub>. Therefore, instead of the valve-switching approach, the ion selection was not applicable to the Rb<sub>1</sub> ion peak, and the  $m/z$  value corresponding to Rb<sub>1</sub> ( $m/z$  1143.6) was eliminated. These strategies significantly reduced interference from the high-abundance PNS components and improved the detection and analysis of the trace saponin components in PNSI



(Fig. 1D).

A detection method of  $[M + Cl]^-$  ion using the MIM mode was developed to simultaneously detect 14 trace saponins in PNSI (Table 1). The MS parameters were optimized using the reference standards. The results showed that the DP values and CXP values were the key parameters when detecting PNS trace components, as shown in Table 1. Other parameters, such as the EP values, CE values, and Dwell time, had negligible effects on the MIM response signals and were set to the default values of  $-10$  V,  $-5$  V, and  $40$  ms, respectively. Our method can achieve simultaneous detection of 18 PNS reference standards (Fig. 2A). Besides, the five main saponins of the PNSIs could also be identified and monitored (gray marks) in the MS spectra. Since the five components have been determined using the conventional UV methods (data not shown), they were not determined in the current study. The peaks of NR<sub>1</sub> (6.8–7.3 min), Rg<sub>1</sub>, and Re (9.1–9.8 min) were removed using the valve-switching strategy. Overall, simultaneous detection of 51 trace saponins in PNSI was achieved (Fig. 2B), and the chromatographic peaks were mainly clustered around 14–20 min. Among them, the  $m/z$  997.5 ion contained the most chromatographic peaks, reaching 11 (Peaks 1, 2, 3, 4, 5, 6, 8, 13, 15, 17, and 22), and all 11 peaks were well-separated in chromatography unit. In addition, in the  $m/z$  655.4 MIM chromatogram, the three main chromatographic peaks at 16–18 min were double charged ions of  $m/z$  1275.6, as  $[M + 2Cl]^{2-}$ , and were the same peaks as those in the  $m/z$  1275.6 chromatogram, so it was not used. In the  $m/z$  967.5, the peaks before peak 7 at 6–8 min was the residuals of NR<sub>1</sub>.

#### Confirmation of ions using EPI mode

The QTRAP instrument was employed to utilize the Enhanced Product Ion Scan (EPI) function on the parent ions after the MIM analysis to obtain the MS/MS spectrum. The EPI mode was subsequently employed to further investigate the structure of trace components that lacked reference standards. For example, in the ion chromatogram of  $m/z$  997.5, the MS/MS spectrum of the peak at 15.62 min exhibited a progressive loss of three glucose molecules ( $-162$  Da) and featured a daughter ion at  $475.1$  Da. These results indicated that the chromatographic peak belonged to the PPT type with three glucose molecules, and thus, the peak was identified as PPT-Glc-Glc-Glc (Fig. S3). Similarly, in the ion chromatogram of  $m/z$  819.5, the MS/MS spectra obtained at the peak of  $17.77$  min displayed the loss of Rha ( $-146$  Da) and Glc ( $-162$  Da) groups, were observed in the MS/MS spectra obtained at the peak of  $17.77$  min, alongside the presence of the  $475.1$  Da daughter ion (Fig. S4). These properties were consistent with the molecular structure of Rg<sub>2</sub>, and the inference was also validated by comparing the obtained data with those of the Rg<sub>2</sub> reference standard.

#### Quantitation based on the standard curve obtained with a similar chemical structure

To quantify the identified trace saponins in PNSI, we prepared a mixed stock solution containing the reference standards of the 18 PNS trace components. This solution was serially diluted into eight different concentrations with a 50%

methanol solution, and the internal standard solution was added at the same concentration. ratio of the peak area of each chromatographic peak to the corresponding internal standard was used to calculate the standard curve. The linear regression analysis was performed to establish the relationship between the ratios and the corresponding concentrations of the reference standards (Table 2). The 18 components to be tested are well linearized in the linear range ( $R^2 > 0.9980$ ). LOD and LOQ were determined as the concentrations of the component yielding a signal-to-noise ratio of 3 and 10, respectively. Remarkably, the LOD for most tested components was as low as  $1 \text{ ng} \cdot \text{mL}^{-1}$  and fell within the linear range of the standard curves.

The standard curves were calculated, and the slope value of each equation was obtained. A scatter plot (Fig. 3) displayed the distribution of each slope along with the corresponding  $[M + Cl]^-$  ions for the reference standards. Except for F<sub>1</sub> and Rh<sub>4</sub>, a linear correlation ( $R^2 = 0.8829$ ) was observed between the  $[M + Cl]^-$  ion and the slope of each reference substance. The unique slope values of F<sub>1</sub> and Rh<sub>4</sub> might be attributed to the C-3 without  $-OH$ . Therefore, the quantitation of trace saponins lacking reference substances was determined using the standard curve sharing the approximate  $[M + Cl]^-$  ion value. For example, in Table 1, the concentrations of the saponins at  $m/z$  967.5 was calculated by referring to the standard curve of noto-K. Meanwhile, the quantitation of saponins at  $m/z$  995.5 and the saponins at  $m/z$  997.5, the latter of which lacked the reference standard, were calculated according to the standard curve of NR<sub>3</sub>. The saponins at  $m/z$  1275.6 and  $m/z$  1407.6 were calculated based on the standard curves of 5,6-didehydro-Rb<sub>1</sub>.

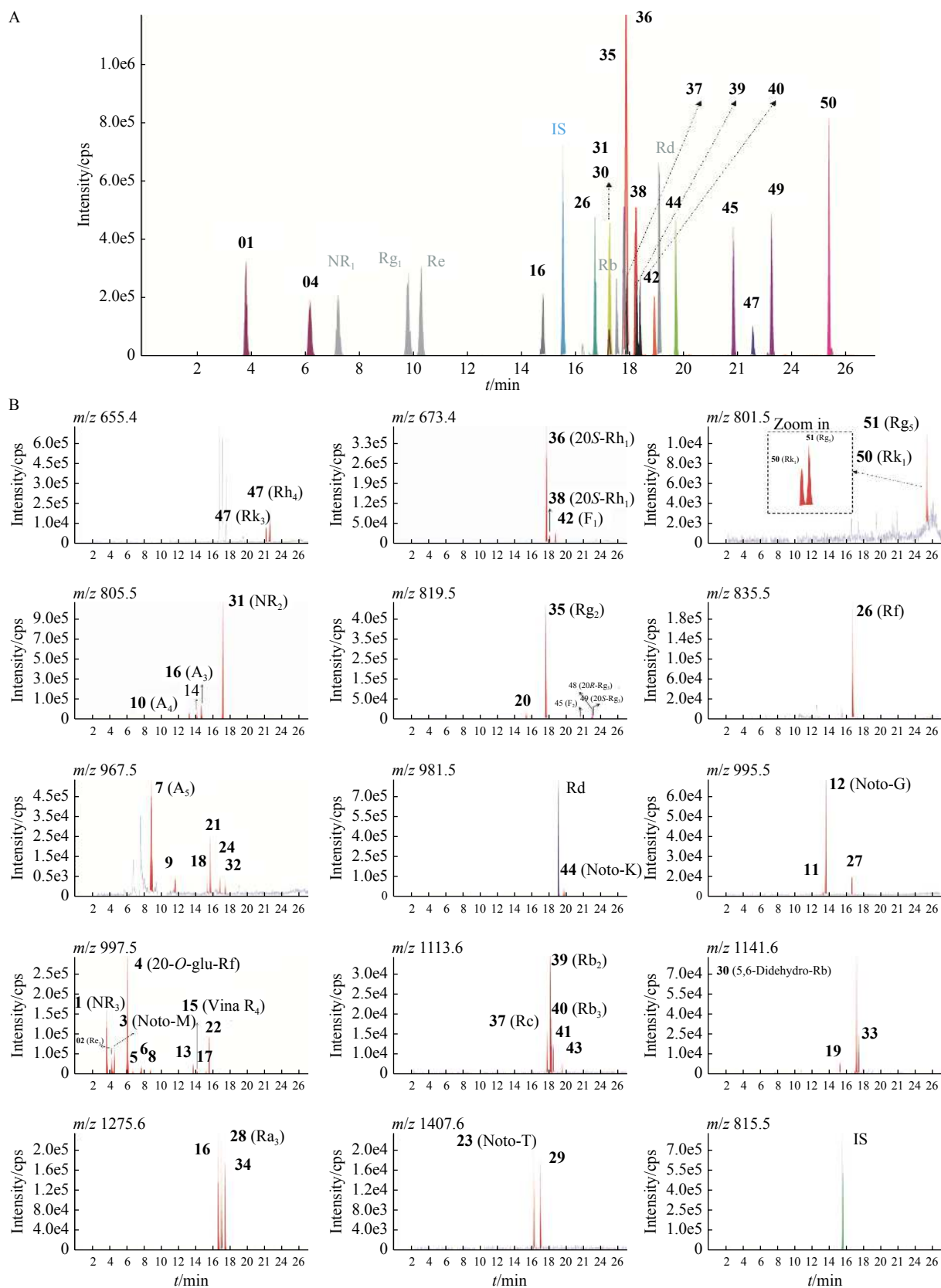
#### Validation

The specificity of the method was evaluated by comparing the chromatographic peaks of the 18 trace saponin reference standards with those extracted from PNSI samples. The retention time was consistent, and the peaks were well resolved, indicating a high degree of method specificity (Fig. 1).

The correlation coefficient values for all 18 saponins were above 0.998, and the lowest points on the regression line corresponded to the LOQ, which was achieved at an impressive level as low as  $1 \text{ ng} \cdot \text{mL}^{-1}$ .

A mixed solution of the 18 trace saponin reference standards was analyzed six times consecutively. The peak area ratios were calculated relative to the internal standard (digoxin). The results showed that the RSD ranged from 4.81% to 9.60%, indicating that the instrument's stability was good (Table 3).

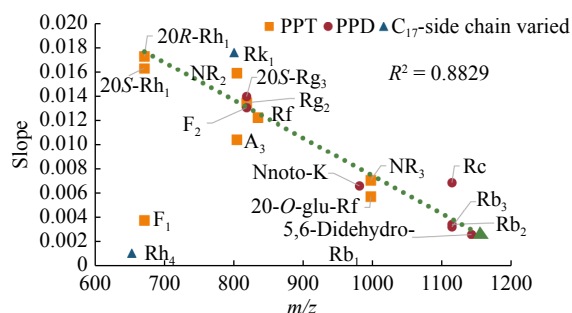
Six preparations were made from the PNSI (lyophilized powder, Vendor 1) to measure the intra-day repeatability of the method. The results were analyzed, and the RSD was 2.64%–10.26%, indicating excellent intra-day repeatability. Inter-day precision was also measured using the PNSI (lyophilized powder, Vendor 1), and the test solution was prepared in triplicates for three consecutive days. The results showed that the RSD was between 3.99% and 13.18%, demonstrating good inter-day repeatability of the method (Table 3).



**Fig. 2** The MIM chromatogram of standards and samples. (A) Overlay MIM chromatogram of 24 saponins standards; (B) MIM chromatogram of PNSI obtained on 14 ions. A total of 51 peaks can be detected

**Table 2** The linear regression analysis of the 18 saponins standards and the LOQ and LOD value

No.	Type	Name	$t_R$ /min	Regression equation	$R^2$	Linear range (ng·mL <sup>-1</sup> )	LOQ (ng·mL <sup>-1</sup> )	LOD (ng·mL <sup>-1</sup> )
1 (01)		Notoginsenoside R <sub>3</sub>	3.86	$Y = 0.007X - 0.022$	0.9986	1.00–500	1.00	0.50
2 (04)		20-Gluco-ginsenoside-Rf	6.22	$Y = 0.006X - 0.011$	0.9998	1.00–499	1.00	0.50
3 (16)		20(S)-Sanchirrhinoside A <sub>3</sub>	14.78	$Y = 0.010X - 0.025$	0.9982	1.27–212	1.27	0.42
4 (26)		Ginsenoside Rf	16.68	$Y = 0.012X - 0.011$	0.9996	1.00–244	0.98	0.49
5 (31)	PPT	20(S)-Notoginsenoside R <sub>2</sub>	17.23	$Y = 0.016X + 0.011$	0.9990	1.49–248	1.49	0.25
6 (35)		Ginsenoside Rg <sub>2</sub>	17.77	$Y = 0.014X + 0.029$	0.9998	1.43–239	1.43	0.24
7 (36)		20(S)-Ginsenoside Rh <sub>1</sub>	17.84	$Y = 0.016X + 0.019$	0.9996	0.99–198	0.99	0.50
8 (38)		20(R)-Ginsenoside Rh <sub>1</sub>	18.19	$Y = 0.017X + 0.008$	0.9994	1.29–216	1.29	0.43
9 (42)		Ginsenoside F <sub>1</sub>	18.87	$Y = 0.004X + 0.002$	0.9998	0.84–421	0.84	0.42
10 (30)		5,6-Didehydroginsenoside Rb <sub>1</sub>	17.21	$Y = 0.003X - 0.012$	0.9988	1.00–496	0.99	0.50
11 (37)		Ginsenoside Rc	17.85	$Y = 0.007X + 0.011$	0.9970	0.49–244	0.49	0.24
12 (39)		Ginsenoside Rb <sub>2</sub>	18.23	$Y = 0.004X + 0.004$	0.9998	1.00–504	1.00	0.50
13 (40)	PPD	Ginsenoside Rb <sub>3</sub>	18.35	$Y = 0.003X + 0.009$	0.9994	1.01–505	1.01	0.51
14 (44)		Notoginsenoside K	19.66	$Y = 0.008X - 0.007$	0.9996	1.00–501	1.00	0.50
15 (45)		Ginsenoside F <sub>2</sub>	21.78	$Y = 0.013X - 0.030$	0.9972	1.00–247	1.03	0.26
16 (49)		20(S)-Ginsenoside Rg <sub>3</sub>	23.18	$Y = 0.014X + 0.002$	0.9998	1.03–259	0.99	0.25
17 (47)	C <sub>17</sub> -side	Ginsenoside Rh <sub>4</sub>	22.50	$Y = 0.001X + 0.002$	0.9968	1.50–150	1.50	0.75
18 (50)	chain varied	Ginsenoside Rk <sub>1</sub>	25.29	$Y = 0.018X + 0.051$	0.9992	1.42–237	1.42	0.24


**Fig. 3** The scatter plot of the slope value of the linear equations obtained by the 18 saponin standards

For the recovery test, the PNSI (lyophilized powder) samples were prepared according to the Method validation section. Half of the lyophilized powder was precisely weighed, and for each of the 18 trace saponins, triplicate samples were prepared with 50%, 100%, and 150% of the expected content. The recovery and RSD were calculated, revealing the recovery rates between 85% and 120% at all three concentration levels, with relative deviations ranging from 1% to 16%. These results confirm that the method meets the analytical criteria (Table 3).

Stability validation of the method was performed by a 24-h continuous analysis of the samples to calculate the RSD of the 18 trace saponin solution. The results revealed that the RSD ranged from 3.25% to 11.02%, indicating that the method exhibited satisfactory stability according to the established criteria.

#### Application to the evaluation of different PNS injections

Quantitative analysis was conducted on 119 batches of PNSIs obtained from seven different manufacturers to assess

the content of 51 trace components (Fig. 4A). Detailed data and scatterplots are shown in Fig. S5. The 119 batches of PNSI samples were divided into five groups (PNSI-1–5, Table S1) based on their types of formulations and manufacturers: PNSI-1, PNSI-2, and PNSI-5 were both prepared by PNS extracted from the taproot of *P. notoginseng*. PNSI-1 was comprised of 60 batches of lyophilized powder of PNSI from Vendor 1, and the total content of the 51 trace saponin components was  $10.2\% \pm 0.8\%$ . PNSI-2 was the liquid preparation of PNSI by the same Vendor 1 as PNSI-1, and the total content of trace saponins was  $16.2\% \pm 1.3\%$  ( $n = 21$ ). PNSI-5 was the liquid injection from other manufacturers (Vendors 5/6/7), and the total content of the trace saponins in PNSI-5 was  $21.0\% \pm 4.5\%$  ( $n = 14$ ). PNSI-3 and PNSI-4 were both PNSIs extracted from the rhizome part of *P. notoginseng*. PNSI-3 comprised lyophilized powder samples from Vendor 2/3, totaling 10 batches, with a total content of trace components of  $14.2\% \pm 1.8\%$ . Liquid injection samples from Vendors 2/3/4 clustered as the PNSI-4 group. The total content of trace saponins in PNSI-4 was  $22.0\% \pm 6.4\%$ . The above results revealed significant variation (10% to 22%) in the total content of trace components among PNSIs of different formulations and manufacturers. Lyophilized powder formulations exhibited the lowest total content (10% to 14%), while injection forms displayed higher levels (16% to 22%). The composition and level variations of trace saponins were not significantly influenced by the source of PNS extraction, whether obtained from *P. notoginseng* taproots or rhizomes. Instead, the processing methods employed by different vendors appeared to be the main contributing factor to the variance in trace components.

A PCA was performed on the quantitative results of the 51 trace saponins to objectively assess the differences among



**Table 3 Method validation: precision and recovery**

No.	Precision			Recovery					
	Instrument	Intra-day	Inter-day	50%		100%		150%	
	RSD%	RSD%	RSD%	%	RSD%	%	RSD%	%	RSD%
1 (01)	6.30	5.69	6.25	111.50	8.91	113.46	8.33	104.77	4.53
2 (04)	6.12	8.17	7.35	99.10	4.60	110.52	6.32	106.95	2.71
3 (16)	7.05	4.04	10.32	96.31	9.43	99.63	8.01	104.25	5.18
4 (26)	5.98	8.89	9.18	95.77	6.18	100.86	7.02	106.71	4.59
5 (31)	6.49	5.49	5.88	92.25	6.22	101.91	6.02	92.40	3.96
6 (35)	6.96	5.42	3.99	95.93	3.42	106.90	11.60	103.62	3.51
7 (36)	7.29	5.70	8.79	104.83	2.77	105.93	2.78	99.44	2.93
8 (38)	6.29	4.33	8.88	90.56	13.03	92.39	7.33	95.25	5.05
9 (42)	7.00	10.26	12.28	117.79	15.72	106.45	11.61	116.01	4.86
10 (30)	6.12	3.60	4.20	95.23	3.04	105.22	7.60	104.58	3.38
11 (37)	7.23	9.99	9.89	88.62	6.48	108.64	10.21	110.34	6.20
12 (39)	9.72	8.85	11.06	92.34	4.29	102.79	3.67	104.38	4.90
13 (40)	9.60	7.63	5.45	90.94	4.45	104.53	3.76	89.25	4.99
14 (44)	6.35	7.30	8.46	103.77	5.42	108.01	5.69	100.89	7.39
15 (45)	5.55	2.64	6.54	119.42	7.03	111.30	5.43	110.27	6.71
16 (49)	4.81	9.31	13.18	119.07	8.07	108.82	5.84	114.58	1.63
17 (47)	6.26	4.94	5.55	109.16	4.60	106.63	3.51	108.64	1.08
18 (50)	6.32	8.01	9.09	86.80	7.44	101.32	4.95	89.30	5.79
Min	4.81	2.64	3.99	86.80	2.77	92.39	2.78	89.25	1.08
Max	9.72	10.26	13.18	119.42	15.72	113.46	11.61	116.01	7.39

the 119 batches of PNSI. The PCA accounted for a cumulative variance contribution rate of 70% from the first two principal components (Fig. 4B). The results revealed distinct clustering patterns. The lyophilized powder PNSI samples (PNSI-1), consisting of 60 batches from Vendor 1, formed a distinct cluster represented by the green circle. Similarly, the liquid solvent PNSI samples (PNSI-2) from the same vendor formed a separate cluster denoted by the blue circle.

In contrast, noticeable overlaps were observed among PNSI-3, PNSI-4, and PNSI-5. The lyophilized powder PNSI-3 samples from Vendor 2/3 clustered together within the red circle, exhibiting similarity to the lyophilized powder PNSI-1 samples from Vendor 1. Furthermore, the liquid injection samples of PNSI-5, derived from the taproot of *P. notoginseng*, showed a significant overlap with those of PNSI-4, extracted from the rhizome portion of *P. notoginseng*, indicating a close compositional relationship between these two groups (Fig. 4B).

Further analysis was performed using the loading plots (Fig. 4C). The distribution of the 51 trace saponins in the loading plots corresponded to the distribution of the 119 PNSI batches observed in the PCA score plot. By comparing the loading plot with the PCA score plot, it was possible to infer the relative content levels of saponins in different groups. Saponins with higher content exhibited a distribution closer to the periphery of the loading plot and occupied a similar position to the corresponding group in the PCA score plot. Conversely, when a saponin's distribution in the loading plot differed from its distribution in the PCA score plot, it indicated relatively lower content levels of that particular saponin in the corresponding group of samples. Besides, the

larger the triangle-shaped legends, the higher the average content of the corresponding saponins in the total saponin injection. The loading plot (Fig. 4C) revealed that the legends of the 34\_Ra<sub>2</sub> isomer, 28\_Ra<sub>3</sub>, and 25\_1275\_1 were larger than those of other components, and their distribution pattern was similar to the sample distribution of PNSI-2 in the score plot (Fig. 4B), indicating that the two components were present in higher amounts in PNSI-2. This finding was consistent with the results shown in Fig. 4A, providing visual confirmation of the elevated levels of these three components in PNSI-2. In contrast, the distribution patterns of 46\_Rk<sub>3</sub> and 47\_Rh<sub>4</sub> closely aligned with those of PNSI-4 and exhibited an inverse relationship with the distribution of PNSI-1, suggesting that the content levels of 46\_Rk<sub>3</sub> and 47\_Rh<sub>4</sub> were the highest in PNSI-4 and the lowest in PNSI-1. Similarly, it was observed that content levels of 39\_Rb<sub>2</sub>, 42\_F<sub>1</sub>, and 44\_noto-K were higher in PNSI-3, PNSI-4, and PNSI-5 but lower in PNSI-1 and PNSI-2 (Fig. 4B).

Therefore, the analysis above showed that the main trace components in PNSI-1 lyophilized powder were Ra<sub>3</sub> isomer (34), Ra<sub>3</sub> (28), 1275-1 (25), and Noto-M (03). The main trace components of PNSI-2 injection from the same manufacturer as PNSI-1, were Rh<sub>4</sub> (47) and Rk<sub>3</sub> (46), Ra<sub>3</sub> isomer (34), Ra<sub>3</sub> (28), and 1275-1 (25). The main trace components of lyophilized powder PNSI-3, contributed by different manufacturers, were Noto-R<sub>2</sub> (31), Rh<sub>4</sub> (47), Ra<sub>3</sub> isomer (34), and Ra<sub>3</sub> (28). The main trace components of PNSI-4 were Rh<sub>4</sub> (47) and Rk<sub>3</sub> (46), 20S-Rh<sub>1</sub> (36), and Noto-R<sub>2</sub> (31); the main trace components of PNSI-5 were Rh<sub>4</sub> (47), Rk<sub>3</sub> (46), 20S-Rh<sub>1</sub> (36), Noto-R<sub>2</sub> (31), and Rg<sub>2</sub> (35).

The results showed visible differences in rare saponins

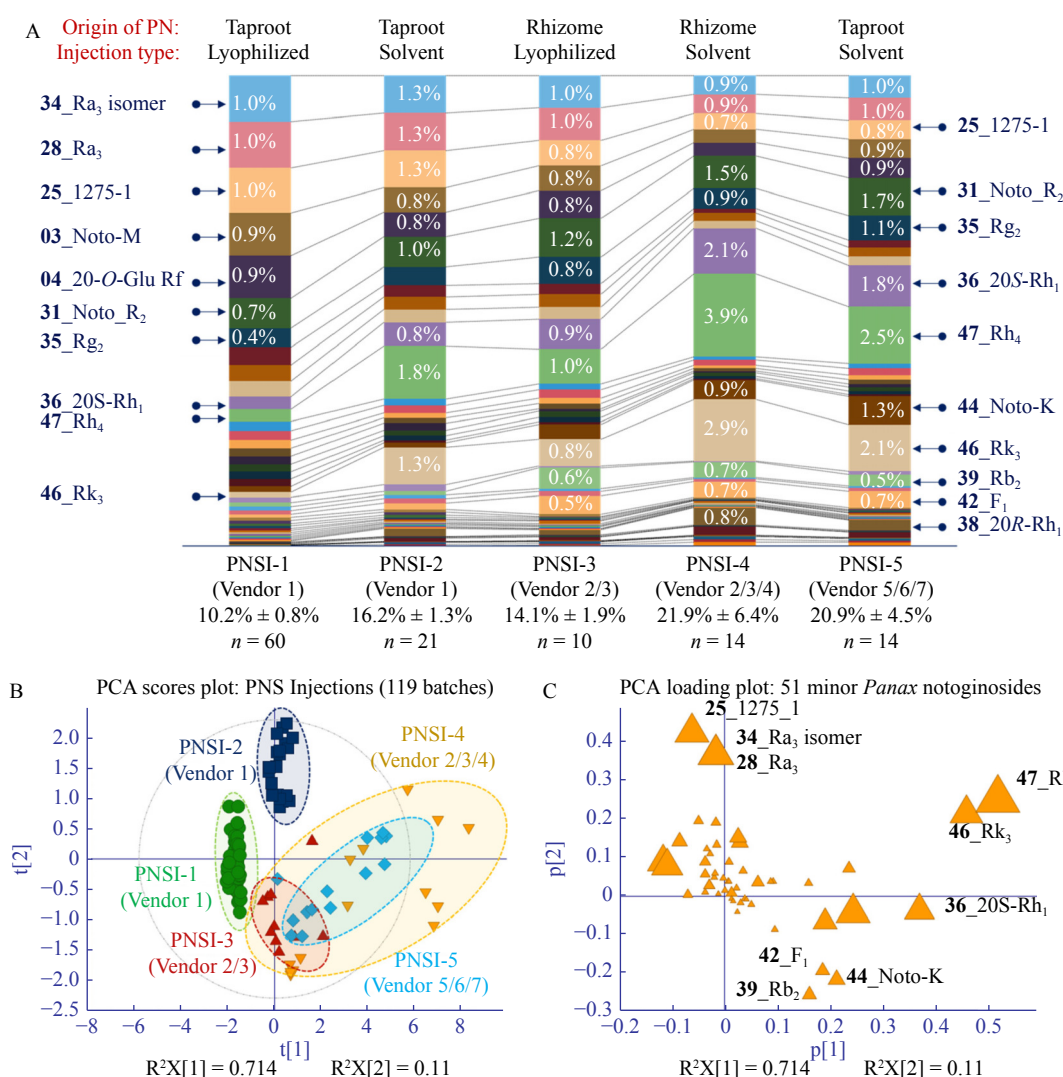


**Fig. 4 Targeted 51 trace ingredients coupled with PCA analysis for consistency evaluation of 119 batches of PNSIs. (A) Stacked column based on the average content of the 51 saponins in different PNSIs; (B) PCA score plot analysis of 119 batches of PNSIs; (C) PCA loading plot analysis of 51 trace saponins**

(like Rk<sub>1</sub> and Rh<sub>5</sub>). The content levels of Rk<sub>1</sub> and Rg<sub>5</sub> in PNSI-1 were hardly detectable, amounting to only 0.004%. Conversely, the content levels of Rk<sub>1</sub> and Rg<sub>5</sub> reached as high as 0.13% in PNSI-4. The differences between PNSI-4 and PNSI-1 denoted an approximately 30-fold difference in content ratios.

For injection solutions, particularly those administered *via* intravenous (i.v.) drip, meticulous quality monitoring is essential to ensure clinical safety. In the case of PNSI-1, the five major saponins (NR<sub>1</sub>, Rg<sub>1</sub>, Re, Rb<sub>1</sub>, and Rd) account for nearly 75%–90% of the total content (data not provided), while the cumulative content of the 51 minor saponin components ranges from 10% to 22% (Fig. S6). This finding indicates that effective quantitative control of most trace saponins in the injection solution has been achieved. Thus, the assessment of these 51 minor saponin components can be employed to evaluate the consistency of injections from the same vendor.

A PCA was performed on 60 batches of PNSI (lyophilized powder) obtained from a single manufacturer (Vendor 1)

to investigate PNSI-1 further. The majority of PNSI samples fell within a stable range (indicated by the red circle), while specific batches exhibited distinct clustering denoted as batch differences (labeled in the green circle) (Fig. S7A). Subsequent PCA biplot (Fig. S7B) and PCA loading plot (Fig. S7C) analyses revealed that Rg<sub>2</sub> (35), noto-R<sub>2</sub> (31), and 20(S)-Rh<sub>1</sub> (36) significantly contributed to the variation observed in these scattered samples. Detailed scatterplot analysis demonstrated a significant reduction in the content levels of these three ginsenosides in the discrete samples (Fig. S7D). Conversely, the content levels of Ra<sub>3</sub> (28), 997-1 (5), 997-2 (6), and 997-3 (8) exhibited corresponding increases. Thus, close monitoring of these anomalous batches is critical for ensuring clinical safety. These findings underscore the necessity of quantifying trace components in herbal preparations, particularly for injection solutions administered *via* i.v. drip.

## Conclusion

PNSIs have an extensive clinical application in China, but their quality control has been limited to monitoring the

five main saponin components (NR<sub>1</sub>, Rg<sub>1</sub>, Re, Rb<sub>1</sub>, and Rd). In this study, we established a quantitative analytical method for 51 trace saponins in PNSIs, utilizing a mixed solution containing 18 trace saponin components as the reference standard. Our method adopted various strategies, including column switching for high-abundance saponins, increased product concentration, and substitute reference standards for trace components to minimize interference. The method was applied to test 119 batches of PNSI products from seven manufacturers, and the tested samples covered two formulations, including lyophilized powder and liquid injection. The results revealed significant variations in trace components between the two formulations, indicating formulation-dependent differences. Moreover, distinct variations in trace saponins were observed among manufacturers, even for the same formulation. For instance, the relative content level of Rh<sub>4</sub> fluctuated between 0.3% and 4.0%, with differences exceeding tenfold between the minimum and maximum limits. Within PNSIs from the same manufacturer, clear patterns of content variation among the 51 trace saponins were identified. In summary, our study presents a more accurate quantitative analytical method to assess the chemical composition of widely used PNSIs in clinical practice. The results offer a fundamental understanding of the overall composition, including the trace saponin components and the quality of the PNSIs distributed in the market from different manufacturers, which will be conducive to the development of more scientifically rigorous approaches for ensuring product consistency and enhancing quality control in the future.

## References

- [1] Long HF, Yang Y, Geng X, *et al.* Changing characteristics of pharmaceutical prices in China under centralized procurement policy: a multi-intervention interrupted time series [J]. *Front Pharmacol*, 2022, **13**: 944540.
- [2] Zhang JL, Cui M, He Y, *et al.* Chemical fingerprint and metabolic fingerprint analysis of Danshen Injection by HPLC-UV and HPLC-MS methods [J]. *J Pharm Biomed Anal*, 2005, **36**(5): 1029-1035.
- [3] Wang H, Chen ML, Li J, *et al.* Quality consistency evaluation of Kudiezi Injection based on multivariate statistical analysis of the multidimensional chromatographic fingerprint [J]. *J Pharm Biomed Anal*, 2020, **177**: 112868.
- [4] Chang Q, Lan LL, Gong DD, *et al.* Evaluation of quality consistency of herbal preparations using five-wavelength fusion HPLC fingerprint combined with ATR-FT-IR spectral quantized fingerprint: belamcandae rhizoma antiviral injection as an example [J]. *J Pharmaceut Biomed Anal*, 2022, **214**: 114733.
- [5] Lin S, Ye J, Zhang WD, *et al.* Development and validation of an analytical method for the determination of flavonol glycosides in ginkgo leaves and Shuxuening Injections by a single marker [J]. *J Chromatogr Sci*, 2016, **54**(6): 1041-1049.
- [6] Wang N, Li ZY, Zheng XL, *et al.* Quality assessment of Kumu Injection, a traditional Chinese medicine preparation, using HPLC combined with chemometric methods and qualitative and quantitative analysis of multiple alkaloids by single marker [J]. *Molecules*, 2018, **23**(4): 856.
- [7] Song Y, Zhang N, Shi S, *et al.* Large-scale qualitative and quantitative characterization of components in Shenfu Injection by integrating hydrophilic interaction chromatography, reversed phase liquid chromatography, and tandem mass spectrometry [J]. *J Chromatogr A*, 2015, **1407**: 106-118.
- [8] Jia M, Zhang B, Qi Y, *et al.* UHPLC coupled with mass spectrometry and chemometric analysis of Kang-ai Injection based on the chemical characterization, simultaneous quantification, and relative quantification of 47 herbal alkaloids and saponins [J]. *J Sep Sci*, 2020, **43**(13): 2539-2549.
- [9] Yang ZR, Wang ZH, Tang JF, *et al.* UPLC-QTOF/MS(E) and bioassay are available approaches for identifying quality fluctuation of Xueshuantong lyophilized powder in Clinic [J]. *Front Pharmacol*, 2018, **9**: 633.
- [10] Guo H, Adah D, James PB, *et al.* Xueshuantong Injection (lyophilized) attenuates cerebral ischemia/reperfusion injury by the activation of Nrf2-VEGF pathway [J]. *Neurochem Res*, 2018, **43**: 1096-103.
- [11] Gao Y, Lyu J, Xie YM, *et al.* Effectiveness and safety of Xueshuantong Injection in treatment of unstable angina pectoris: a systematic review and meta-analysis of randomized controlled trials [J]. *Chin J Chin Mater Med*, 2019, **44**(20): 4366-4378.
- [12] Tang XG, Huang MD, Jiang JS, *et al.* *Panax notoginseng* preparations as adjuvant therapy for diabetic kidney disease: a systematic review and meta-analysis [J]. *Pharm Biol*, 2020, **58**(1): 138-145.
- [13] Zhang J, Guo F, Zhou R, *et al.* Proteomics and transcriptome reveal the key transcription factors mediating the protection of *Panax notoginseng* saponins (PNS) against cerebral ischemia/reperfusion injury [J]. *Phytomedicine*, 2021, **92**: 153613.
- [14] Liu L, Zhang Q, Xiao S, *et al.* Inhibition of shear-induced platelet aggregation by Xueshuantong via targeting Piezo1 channel-mediated Ca<sup>2+</sup> signaling pathway [J]. *Front Pharmacol*, 2021, **12**: 606245.
- [15] Zhou D, Cen K, Liu W, *et al.* Xuesaitong exerts long-term neuroprotection for stroke recovery by inhibiting the ROCKII pathway, *in vitro* and *in vivo* [J]. *J Ethnopharmacol*, 2021, **272**: 113943.
- [16] Zhang HY, Niu W, Olaleye OE, *et al.* Comparison of intramuscular and intravenous pharmacokinetics of ginsenosides in humans after dosing Xueshuantong, a lyophilized extract of *Panax notoginseng* roots [J]. *J Ethnopharmacol*, 2020, **253**: 112658.
- [17] Liu H, Lu X, Hu Y, *et al.* Chemical constituents of *Panax ginseng* and *Panax notoginseng* explain why they differ in therapeutic efficacy [J]. *Pharmacol Res*, 2020, **161**: 105263.
- [18] Yao CL, Yang WZ, Zhang JX, *et al.* UHPLC-Q-TOF-MS-based metabolomics approach to compare the saponin compositions of Xueshuantong Injection and Xuesaitong Injection [J]. *J Sep Sci*, 2017, **40**(4): 834-841.
- [19] Yu Y, Yao C, Guo DA. Insight into chemical basis of traditional Chinese medicine based on the state-of-the-art techniques of liquid chromatography-mass spectrometry [J]. *Acta Pharm Sin B*, 2021, **11**(6): 1469-1492.
- [20] Cheng X, Li X, Liao B, *et al.* Improved performance of proteomic characterization for *Panax ginseng* by strong cation exchange extraction and liquid chromatography-mass spectrometry analysis [J]. *J Chromatogr A*, 2023, **1688**: 463692.
- [21] Liang Y, Guan TY, Zhou YY, *et al.* Effect of mobile phase additives on qualitative and quantitative analysis of ginsenosides by liquid chromatography hybrid quadrupole-time of flight mass spectrometry [J]. *J Chromatogr A*, 2013, **1297**: 29-36.

**Cite this article as:** ZHANG Jingxian, ZHANG Zijia, WANG Zhaojun, ZHANG Tengqian, ZHOU Yang, CHEN Ming, HUANG Zhanwen, HE Qingqing, LONG Huali, HOU Jinjun, WU Wanying, GUO Dean. Targeted trace ingredients coupled with chemometric analysis for consistency evaluation of *Panax notoginseng* saponins injectable formulations [J]. *Chin J Nat Med*, 2023, 21(8): 631-640.